

Quantitative Image Quality Measurements of a Digital Breast Tomosynthesis System

Quantitative Messungen der Bildqualität an einem digitalen Brusttomosynthesesystem

Authors

T. Olgar¹, T. Kahn², D. Gosch²

Affiliations

¹ Faculty of Engineering, Department of Engineering Physics, Ankara University, Ankara

² Department of Diagnostic and Interventional Radiology, University of Leipzig, Leipzig

Key words

- ◉ image quality
- ◉ detective quantum efficiency
- ◉ digital breast tomosynthesis
- ◉ modulation transfer function
- ◉ noise power spectrum

eingereicht 26.11.2012

akzeptiert 29.5.2013

Bibliography

DOI <http://dx.doi.org/10.1055/s-0033-1350106>
 Published online: 25.7.2013
 Fortschr Röntgenstr 2013; 185: 1188–1194 © Georg Thieme Verlag KG Stuttgart · New York · ISSN 1438-9029

Correspondence

Dr. Dieter Gosch
 Klinik und Poliklinik für Diagnostische und Interventionelle Radiologie, Universitätsklinikum Leipzig AöR
 Liebigstraße 20
 04103 Leipzig
 Germany
 Tel.: 03 41/9 71 74 16
 Fax: 03 41/9 71 74 09
 gosd@medizin.uni-leipzig.de

Zusammenfassung



Ziel: Das Ziel der Studie war die quantitative Messung der Bildqualität an einem Brusttomosynthesesystem.

Material und Methoden: Die Signalübertragungseigenschaften (STP), die Modulationsübertragungsfunktion (MTF), das Rauschspektrum (NPS) und die detektive Quantenausbeute (DQE) wurden nach etablierten Methoden an einem Brusttomosynthesesystem Selenia Dimensions von Hologic gemessen. Das NPS wurde mittels zweidimensionaler (2-D) schneller Fouriertransformation (FFT) aus Flatfieldbildern berechnet. Die presampling MTF des Systems wurde mittels der Kantenmethode für 2-D-Standardprojektionsaufnahmen und für den 3-D-Brusttomosynthesemodus ermittelt. Die DQE wurde für unterschiedliche Detektordosiswerte (DAK) aus den gemessenen NPS und MTF abgeleitet.

Ergebnisse: Die Detektorresponsfunktion war linear für die 2-D-Standardprojektionsaufnahmen und für den 3-D-Brusttomosynthesemodus. Der Gradient der Detektorrespons im 3-D-Aufnahmemodus war um den Faktor 3,1 höher als im 2-D-Aufnahmebetrieb. Die bei der Nyquist-Frequenz gemessenen MTF-Werte waren 32% im 2-D-Modus und 39% im 3-D-Modus. Die Sättigung der DQE im 3-D-Modus erfolgte bei Luftkermawerten, die um den Faktor 3,5 niedriger waren als im 2-D-Modus. Der gemessene maximale DQE-Wert lag bei 54%.

Schlussfolgerung: Die gemessenen DQE-Werte waren vergleichbar mit denen von Brusttomosynthesesystemen anderer Hersteller (Siemens, GE).

Abstract



Purpose: The aim of this study was to measure the image quality of a digital breast tomosynthesis (DBT) system quantitatively.

Materials and Methods: The signal transfer property (STP), modulation transfer function (MTF), noise power spectrum (NPS), and detective quantum efficiency (DQE) of the Hologic Selenia Dimensions breast tomosynthesis system were measured according to established methods. The NPS was calculated from two-dimensional (2D) fast Fourier transform (FFT) of flat field images. The presampling MTF of the system was determined for 2D standard projection mammography and 3D breast tomosynthesis mode using the edge method. The DQE was derived for different detector air kerma (DAK) values from NPS and MTF measurements.

Results: The detector response function was linear for both two-dimensional (2D) standard projection mammography and three-dimensional (3D) breast tomosynthesis modes. The gradient of the detector response in the 3D imaging mode was higher than the gradient in the 2D imaging mode by a factor of 3.1. The MTF values measured at the Nyquist frequency were 32% and 39% in 2D and 3D imaging modes, respectively. The DQE was saturated at an air kerma value approximately 3.5 times lower in 3D mode than in 2D mode. The measured maximum DQE value was 54%.

Conclusion: The measured DQE values were comparable with breast tomosynthesis systems from other companies (Siemens, GE).

Citation Format:

► Olgar T, Kahn T, Gosch D. Quantitative Image Quality Measurements of a Digital Breast Tomosynthesis System. Fortschr Röntgenstr 2013; 185: 1188–1194

Introduction

Digital breast tomosynthesis (DBT) is a 3 D imaging technique that can reduce or eliminate the tissue overlap effect. During tomosynthesis, the X-ray gantry rotates and acquires projections of the stationary compressed breast at multiple angles [1]. The projection images are then reconstructed into a series of thin-slice images. Breast tomosynthesis systems have been developed by different manufacturers, and an increasing number of studies compare the clinical performance of FFDM and DBT [2, 3]. There are also some recent publications dealing with the dosimetric properties of DBT for the 2 D conventional mammography and 3 D breast tomosynthesis modes [4, 5].

Image quality can be assessed subjectively or quantitatively [6–8]. Subjective image quality assessment is observer-dependent, and the observer can be adapted to the simulated objects in the phantoms used in the measurements. Therefore, quantitative image quality measurements with established standards give more realistic results than visual methods.

Quantitative image quality of the digital system can be measured in terms of detector response or signal transfer property (STP), modulation transfer function (MTF), noise power spectrum (NPS) and detective quantum efficiency (DQE). The MTF is used to describe the resolution properties and the NPS is used to characterize the magnitude of the noise of an imaging system in the spatial frequency domain. A higher MTF means better image sharpness and resolution, and the lower the NPS, the lower the noise within of radiographic image. The DQE is always derived from MTF and NPS measurements to quantify the overall image quality and compare the performance of different image detectors quantitatively. The DQE is defined as the efficiency of the imaging detector in transferring the signal-to-noise ratio (SNR) from an input to an output. The detectability of low-contrast objects is highly dependent on the imaging system's SNR and the magnitude of noise. To increase detectability of low-contrast lesions, the SNR should be increased, whereas image noise should be reduced as much as possible, as an ideal detector DQE is equal to unity at all spatial frequencies [9]. In practice, the SNR at the output of the imaging system is always lower than the input, and the DQE value of an imaging system is always less than unity. The higher the DQE, the more X-ray photons interacting with the imaging detector are used to produce an image.

The IEC62 220–1-2 standard was introduced in 2007 to standardize imaging geometry and beam quality in DQE measurements for digital mammography systems [10]. The implementation of this standard permits the comparison of the DQE among different imaging detectors. Several studies have reported image quality measurement results for different breast tomosynthesis systems [11–15]. Most of these studies were carried out using a Siemens Mammomat prototype tomosynthesis system (Siemens, Erlangen, DE). To our knowledge, the first physical image quality measurements for the Selenia Dimensions breast tomosynthesis system were carried out by Hologic employees [16, 17]. Marshall and Bosmans recently published a study of system sharpness measurement (MTF) comparing Siemens Inspiration and Hologic Selenia Dimensions DBT systems [18].

Our study characterizes the MTF, NPS and DQE of an amorphous selenium-based Hologic Selenia Dimensions breast tomosynthesis system using established methods. The DQE was measured for different detector air kerma values and compared with published results from other breast tomosynthesis systems.

Materials and methods

The Selenia Dimensions (Hologic, USA) digital mammography system can be used both for 2 D conventional mammography and 3 D breast tomosynthesis [16]. The Selenia Dimensions image detector is based on direct capture amorphous selenium technology and has a detector pixel size of $70\ \mu\text{m}$. The detector is operated in full resolution mode with a pixel size of $70\ \mu\text{m}$ in 2 D mode and 2×2 binning with a pixel size of $140\ \mu\text{m}$ in 3 D mode. In 2 D imaging mode, an anti-scatter high transmission cellular (HTC) grid which automatically moves out of the field of view when 3 D imaging mode is used. The X-ray tube has a tungsten (W) anode with additional filtration of $50\ \mu\text{m}$ rhodium (Rh), $50\ \mu\text{m}$ silver (Ag) and $0.7\ \text{mm}$ aluminum (Al). The Rh or Ag X-ray filter is used in the 2 D imaging mode, and the Al filter in the 3 D imaging mode. During breast tomosynthesis the system acquires 15 projection images in increments of approximately 1° starting at -7.5° and ending with $+7.5^\circ$, with the breast in standard compression. The focus detector distance is $70\ \text{cm}$, and the breast support plate is $2.5\ \text{cm}$ above the detector surface. The acquired image of the breast at different angles is reconstructed by using a specialized filtered back projection method [16, 17].

The first step of the quantitative image quality measurements is the determination of the detector response, which gives the relationship between the mean pixel value (PV) and the detector air kerma. The detector air kerma was measured with a calibrated dosimeter (UNIDOS webline, PTW Freiburg, Germany) and a mammographic ion chamber (SFD Chamber Type 34 069, PTW Freiburg, Germany). The accuracy of dose measurements was 5%. The dose was measured as a function of mAs with 28 kVp, W/Rh target filter in 2 D standard projection mammography mode and W/Al target filter setting in 3 D breast tomosynthesis mode. Detector response measurement was carried out with flat field zero degree tomo mode, and the mean pixel value was taken from the first image of the tomography sequence to reduce the lag effect in 3 D breast tomosynthesis mode. In this mode, the X-ray tube was stationary during image acquisition. Individual DBT projection images in 3 D breast tomosynthesis mode were extracted from archive files using “gexpand” and “mview” decoding software provided by Hologic Corp. The detector response was measured following the geometry described in IEC protocol for mammography and high purity (99.9%) $2\ \text{mm}$ Al added filtration to the beam [10]. The mean pixel value was extracted from a region of interest (ROI) of 256×256 pixels placed at the distance of $60\ \text{mm}$ from the chest wall edge. The PV was then plotted against the detector air kerma (DAK). The detector response curve is used to normalize and linearize the images used for the calculation of MTF and NPS.

The standard deviation (SD) of the PV within the ROI was also recorded during detector response measurement in order to investigate quantum limited operation of the detector. The SNR was calculated from the measured mean pixel value and the SD of the PV within the ROI, and the SNR^2 was plotted against the detector air kerma. The linearity of this curve was established by plotting a best fit through all measured points [19].

The presampling MTF is measured using the edge method as described elsewhere [20]. The edge test device consists of a $1\ \text{mm}$ thick, $120\ \text{mm}$ long and $60\ \text{mm}$ wide stainless steel plate. The edge was placed on the breast support plate with the edges angled approximately 3° to the pixel matrix during measurement. The edge spread function (ESF) of the system was defined as the pixel value versus the perpendicular distance from the

edge transition. The ESF was then differentiated to obtain the line spread function (LSF). Finally, the MTF was calculated via Fourier transformation of the LSF. The images for MTF calculation were acquired at 28 kVp using a W/Rh target/filter combination and without additional filtration or grid in the 2D standard projection mammography mode. The same exposure condition was used in 3D mode but with a W/Al target filter combination. The MTF was measured for both c-arm scanning (tube-travel direction) and front-back (chest wall-nipple direction) directions. In the results section, only the MTF in the scanning direction is reported because of small differences between the MTF results and to show the overall system performance.

The NPS was calculated from the detector response images using previously published methods [21–23]. Sub-images of 1024×1024 pixels were extracted from the central region of the flat field images and linearized to air kerma using the response curve. A 2D second-order polynomial surface was fitted and then subtracted from this region in order to remove low frequency background trends such as the anode-heel effect from the X-ray source on the NPS. Half overlapped (by 64 pixels in each direction), regions of interest (ROIs) of 128×128 pixels were selected from the sub-image. In this manner, a total of 128 ROIs were used in the NPS measurements. The NPS was calculated by implementation of 2D fast Fourier transform (FFT) to each ROI using software developed by NHSBSP [24]. One dimensional (1D) NPS was obtained from 2D NPS by averaging central ± 7 rows or columns (including the axis) around each axis. The normalized noise power spectrum (NNPS) was then calculated by dividing by the square of the mean PV of the linearized sub-image. DQE can be calculated from the measured MTF and NNPS as follows:

$$DQE(u) = \frac{(SNR)_{out}^2}{(SNR)_{in}^2} = \frac{MTF^2(u)}{q \cdot DAK \cdot NNPS(u)}$$

where $MTF(u)$ is the measured pre-sampling MTF in the u direction (the tube scanning direction in this study), DAK is the measured air kerma at the detector plane for flat field image acquisition, $NNPS(u)$ is the normalized noise power spectrum in the u direction and q is the number of photons per unit air kerma per mm^2 for the X-ray beam quality used in the NNPS and detec-

tor response measurements [25]. The factor q is calculated from the software MIQuaELa v.1.0 package [26, 27].

Results



The detector response curve for each imaging mode is given in **Fig. 1**. The detector response function was linear for both 2D and 3D imaging modes. The gradient of the detector response in 3D imaging mode was higher by a factor of 3.1 than the gradient in 2D imaging mode. **Fig. 2** shows the relationship between SNR² and detector air kerma in 2D and 3D imaging modes. The linearity of the curves was very good for both 2D and 3D imaging modes. Non-linearity shows the presence of additional noise sources besides quantum noise [19].

Fig. 3 illustrates the measured presampling MTF for the static flat field conventional 2D mode (pixel size 0.07 mm), static flat field zero degree tomo mode (pixel size 0.14 mm), scanning flat field tomo mode (pixel size 0.14 mm) and reconstructed edge image with pixel size of 0.1 mm.

The MTF values measured at the Nyquist frequency (7.14 and 3.57 cycles/mm in 2D and 3D imaging modes, respectively) were 32% and 39% in 2D and 3D imaging modes, respectively. The decrease in MTF for the oblique incidence of X-rays on the detector in scanning mode of the DBT system was also investigated. The decrease in MTF for the maximum angle (7.5° for the breast tomosynthesis system used in this study) was less than 3% because of the narrow scanning angle range used in this study compared to other breast tomosynthesis systems developed by different companies.

The results of NNPS measurements for 2D and 3D imaging modes are illustrated in **Fig. 4**, **Fig. 5**. **Fig. 6**, **7** demonstrate the measured DQE for 2D and 3D imaging modes, respectively. The calculated maximum DQE value was 54% for both 2D and 3D imaging modes.

Discussion



In this study, the image quality of the Hologic Selenia Dimensions breast tomosynthesis system was measured quantitatively.

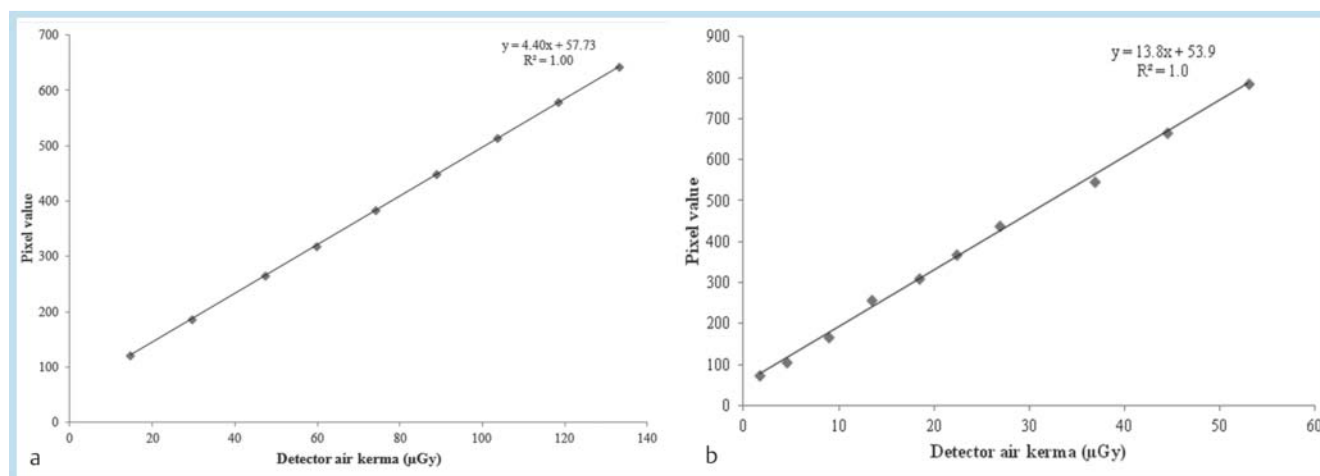


Fig. 1 **a** Detector response curve for 2D imaging mode. **b** Detector response curve for 3D imaging mode.

Abb. 1 **a** Detektorresponskurve für den 2-D-Aufnahmemodus. **b** Detektorresponskurve für den 3-D-Aufnahmemodus.

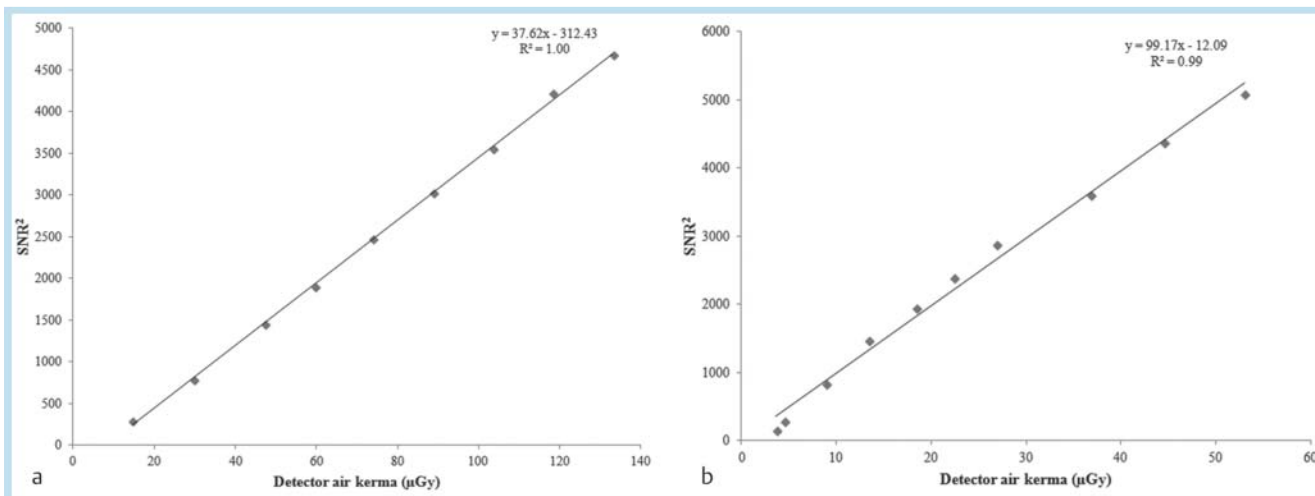


Fig. 2 a SNR² against detector air kerma for 2 D imaging mode. b SNR² against detector air kerma for 3 D imaging mode.

Abb. 2 a SNR² als Funktion der Luftkerma am Detektor für den 2-D-Aufnahmemodus. b SNR² als Funktion der Luftkerma am Detektor für den 3-D-Aufnahmemodus.

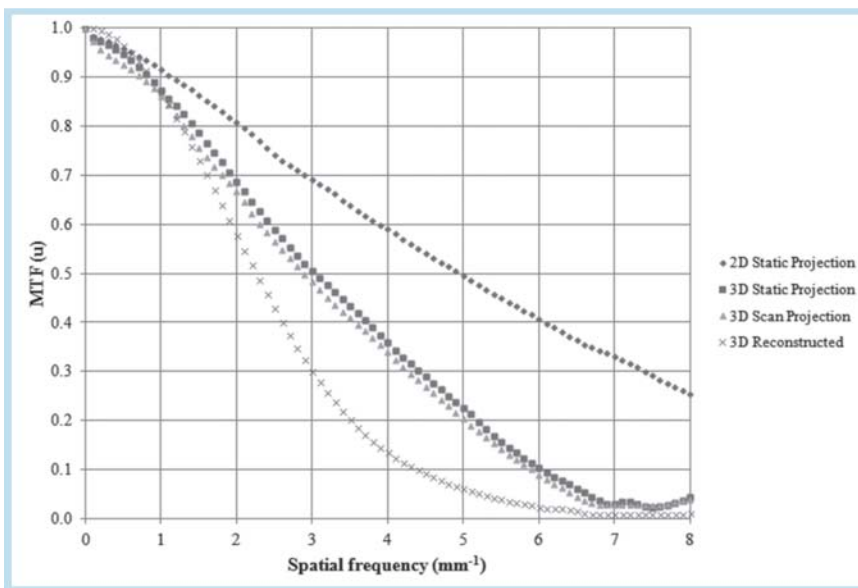


Fig. 3 MTFs for various imaging modes.

Abb. 3 MTF für verschiedene Aufnahmemodi.

Quantitative image quality measurements have been published for various breast tomosynthesis systems. However, only a few studies focused on the breast tomosynthesis system used in this study.

The detector response curves established in our study were linear and similar to the curves reported by Marshall et al. for the Siemens Mammomat InspirationTomo [11]. Many digital imaging systems demonstrate linear response curves (e.g., flat panel X-ray imaging systems), while some have logarithmic response curves (e.g. photostimulable phosphor detector systems). A detector having logarithmic response produces a signal more directly related to the tissue composition along the path, due to the exponential attenuation of X-rays. Logarithmic transformation can be applied to the detector data with the effect of reducing the range of the signal [28]. However, in order to make meaningful calculations, the relationship between system input and output should be linear. If the STP is logarithmic or a power

law, all the image data should be linearized by applying the inverse of the STP to each pixel value [29]. Marshall et al. reported that the gradient of the detector response for the DBT mode was higher than the 2D imaging mode by a factor of 3.5. In this study, we measured a detector response gradient in DBT mode 3.1 times greater than that in 2D mode because of the 3D mode operated with 2×2 pixel binning and with a higher electronic gain. This allows a fast readout, suppression of other electronic noise after pre-amplification and the usage of a more dynamic range of the detector, resulting in signal saturation at lower detector air kerma values [16].

Our MTF measurement results for different imaging modes were also similar to Marshall and Bosmans's results for the same breast tomosynthesis system used in this study [18]. They reported MTFs for 2.0 and 4.0 spatial frequencies of approximately 0.78 and 0.60 for the planar mammography (2D), 0.60 and 0.22 for DBT scan mode, and 0.58 and 0.12 for the reconstructed planes

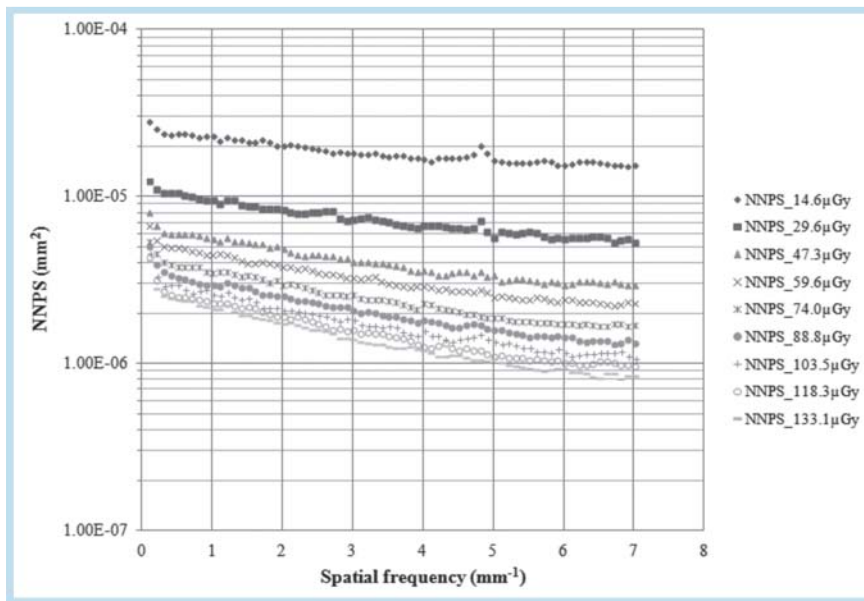


Fig. 4 Measured NNPS for different DAK values in 2D imaging mode.

Abb. 4 Gemessene NNPS für verschiedene DAK-Werte im 2-D-Aufnahmemodus.

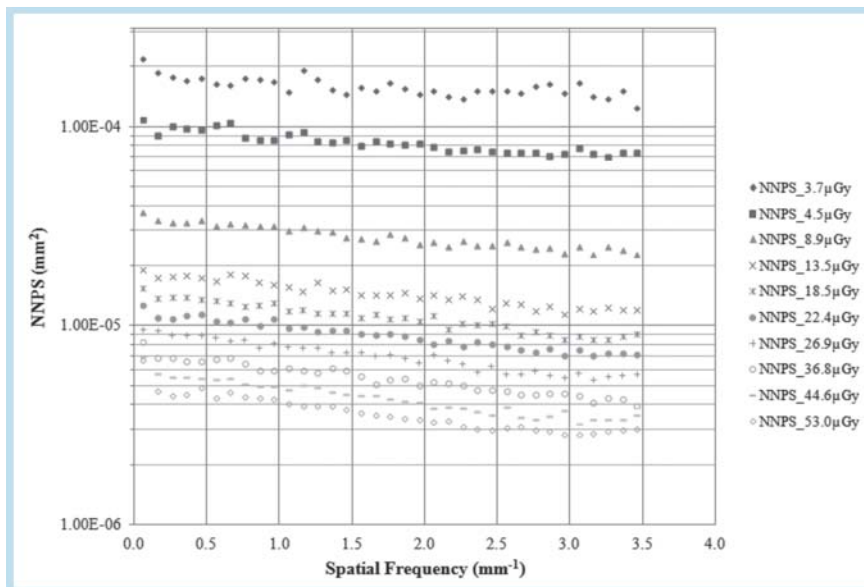


Fig. 5 Measured NNPS for different DAK values in 3D imaging mode.

Abb. 5 Gemessene NNPS für verschiedene DAK-Werte im 3-D-Aufnahmemodus.

in left-right (LR) direction, respectively. The measured MTFs for the same spatial frequencies in our study were 0.81 and 0.59 for 2D, 0.66 and 0.34 for DBT scan, and 0.58 and 0.13 for the reconstructed plane in the LR direction, respectively. Our MTFs were also comparable to results from Baorui et al. for the prototype Hologic breast tomosynthesis system [17].

The measured NNPS in this study was comparable to the NNPS measured by Marshall et al. for Siemens Mammomat Inspiration-Tomo [11]. Their NNPS value at 2.0 spatial frequency and 23.9 μGy DAK value is approximately 1.0×10^{-5} in DBT scan mode and 3.0×10^{-6} at 98.0 μGy DAK value in 2D mode. In this study, we calculated an NNPS of 8.32×10^{-6} at 22.4 μGy DAK value and 2.12×10^{-6} at 103.5 μGy DAK value in DBT scan tomo mode and 2D mode, respectively.

In this study, the calculated DQE was saturated at approximately 13.5 μGy in 3D scan tomo mode and between 47.3 and 74.0 μGy in 2D planar mammography mode. The DQE was saturated at a lower DAK value in 3D imaging mode due to the higher gradient

of the detector in this mode. The established maximum DQE value was 54% for both 2D and 3D imaging modes. The maximum DQE value was decreased for higher DAK values at lower frequencies in the 2D imaging mode. The gain map acquired at lower detector pixel counts failed at higher counts. After gain correction of the high count images, more artifacts could be detected. At lower frequencies, these artifacts increased and the DQE dropped. For normal 2D breast imaging, the detector rarely measures above 1000 counts. The average level is about 500 counts in 2D imaging mode. The flat field gain map used for correction at this level results in the best image quality. A correct DQE measurement at higher count levels should be performed with a new gain map.

Baorui et al. reported higher DQE values for the same breast tomosynthesis system used in this study [16]. They measured the DQE without a detector cover, and the difference in DQE values can be attributed to the detector cover used during DQE measurement in our study. The DQE value saturated at lower DAK values (9.43 μGy in 3D and between 48.8 and 73.3 μGy in 2D

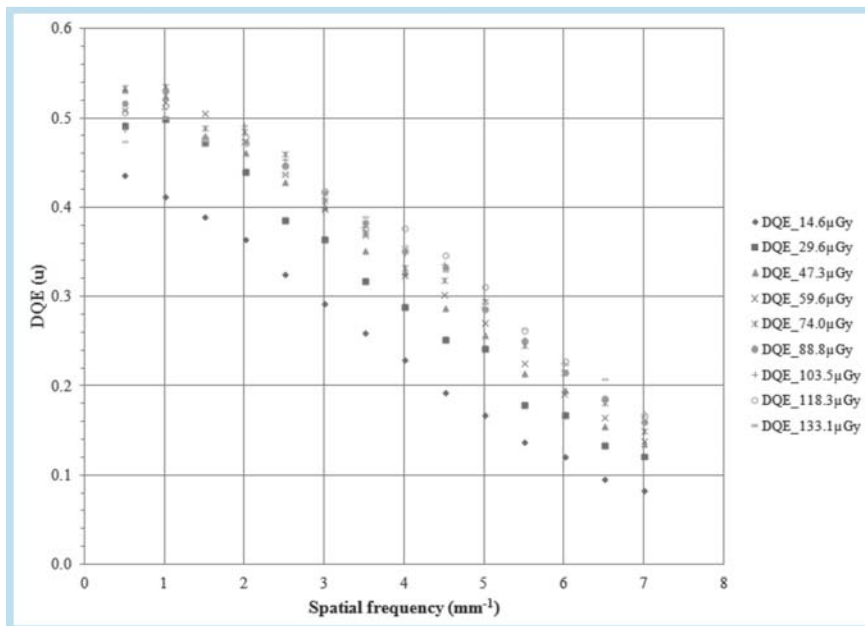


Fig. 6 Derived DQE for different DAK values in 2-D imaging mode.

Abb. 6 Abgeleitete DQE für verschiedene DAK-Werte im 2-D-Aufnahmemodus.

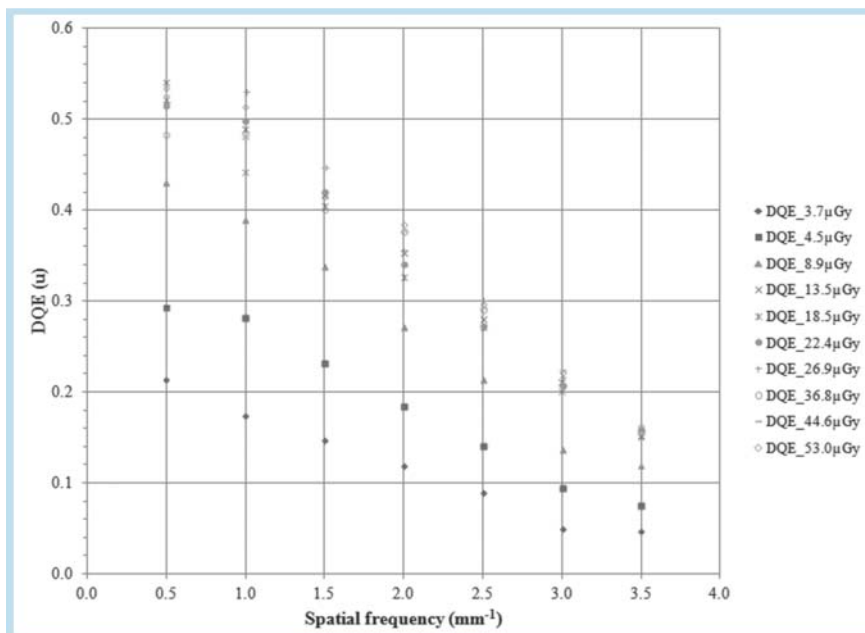


Fig. 7 Derived DQE for different DAK values in 3-D imaging mode.

Abb. 7 Abgeleitete DQE für verschiedene DAK-Werte im 3-D-Aufnahmemodus.

mode) in the study by Baorui et al. because the calculated DAK value at the detector surface in our study is approximately 10% higher. We measured air kerma values used in DQE calculation above the breast support plate, which resulted in an overestimation of the air kerma value at the detector entrance. This situation in turn will lead to an underestimation of the calculated DQE for a specific air kerma value by the reciprocal of the transmission of the breast support table in terms of air kerma [22]. Choi et al. measured the physical image quality and evaluated the clinical performance of the prototype DBT system developed by KERI (Korea Electrotechnology Research Institute) and reported a maximum DQE for the full resolution and 2×2 pixel binning modes as 47.09% and 50.24%, respectively [30, 31]. Zaho et al. reported closer DQE values for the prototype of Siemens Mammomat Novation^{DR}. They established DQE values for both full resolution (pixel size 85 μm) and binning mode (pixel

size 170 μm in the tube travel direction) at DAK values between 3.6–50 μGy. They described a maximum DQE value around 55%, which is in good agreement with our findings [13]. Bissonnette et al. have also reported comparable DQE values for the Siemens Mammomat Novation^{DR} at 2.3–43.6 μGy detector air kerma range [15]. Varjonen estimated the DQE for a prototype GE Diamond DX breast tomosynthesis system in the 7–136 μGy DAK range. She measured the MTF with a slit phantom and established the DQE using a 28 kVp, Mo/Mo target/filter combination and 4 cm PMMA included in the beam path. Her result for the maximum DQE value is higher than our results [14]. This difference may have resulted from the beam quality and the different MTF measurement method used in her study.

Conclusion

This paper reports detailed measurements of quantitative image quality of a Hologic Selenia Dimensions breast tomosynthesis system. The measured DQE values for different detector air kermas were comparable with breast tomosynthesis systems from Siemens and GE.

Acknowledgement

This study was supported by the TUBITAK (The Scientific and Technological Research Council of TURKEY) under the program No: 2219. T Olgar would like to thank Baorui Ren from Hologic Corp. for useful scientific and technical discussions.

References

- 1 Park JM, Franken EA Jr, Garg M et al. Breast Tomosynthesis: Present considerations and future applications. *RadioGraphics* 2007; 27: 231–240
- 2 Teertstra HJ, Loo CE, van den Bosch MA et al. Breast tomosynthesis in clinical practice: initial results. *Eur Radiol* 2010; 20: 16–24
- 3 Gennaro G, Toledano A, di Maggio C et al. Digital breast tomosynthesis versus digital mammography: a clinical performance study. *Eur Radiol* 2010; 20: 1545–1553
- 4 Olgar T, Kahn T, Gosch D. Average Glandular Dose in Digital Mammography and Breast Tomosynthesis. *Fortschr Röntgenstr* 2012; 184: 911–918
- 5 Feng SS J, Sechopoulos I. Clinical Digital Breast Tomosynthesis System: Dosimetric Characterization. *Radiology* 2012; 263: 35–42
- 6 Blendl C, Schreiber AC, Buhr H. Results of an Automatic Evaluation of Test Images according to PAS 1054 and IEC 6220-1-2 on Different Types of Digital Mammographic Units. *Fortschr Röntgenstr* 2009; 181: 979–988
- 7 Obenauer S, Hermann KP, Schorn C et al. Full-field digital mammography: Dose-dependent detectability of simulated breast lesions. *Fortschr Röntgenstr* 2000; 172: 1052–1056
- 8 Schulz-Wendtland R, Wenkel E, Lell M et al. Experimental phantom lesion detectability study using a digital breast tomosynthesis prototype system. *Fortschr Röntgenstr* 2006; 178: 1219–1223
- 9 Samei E. Performance of Digital Radiographic Detectors: Quantification and Assessment Methods. *Advances in Digital Radiography*. RSNA Categorical Course in Diagnostic Radiology Physics 2003: 37–47
- 10 IEC (International Electrotechnical Commission). Medical electrical equipment characteristics of digital x-ray imaging devices-part 1.2. Determination of detective quantum efficiency—Detectors used in mammography IEC 62220-1-2. Geneva: International Electrotechnical Commission; 2007
- 11 Marshall NW, Jacobs J, Cockmartin L et al. Technical evaluation of a digital breast tomosynthesis system. *IWDM 2010*, LNCS 6136, 350–356
- 12 Zhao B, Zhao J, Hu YH et al. Experimental validation of a three-dimensional linear system model for breast tomosynthesis. *Med. Phys* 2009; 36: 240–251
- 13 Zhao B, Zhao W. Imaging performance of an amorphous selenium digital mammography detector in a breast tomosynthesis system. *Med Phys* 2008; 35: 1978–1987
- 14 Varjonen M. Three-Dimensional (3D) Digital Breast Tomosynthesis (DBT) in the Early Diagnosis and Detection of Breast Cancer. Doctoral dissertation. 2006, ISBN 952-15-1584-8 <http://URN.fi/URN:NBN:fi:tty-200810021130>
- 15 Bissonnette M, Hansroul M, Masson E et al. Digital breast tomosynthesis using an amorphous selenium flat panel detector. *Proc. of SPIE* 2005; 5745: 529–540
- 16 Ren B, Ruth C, Wu T et al. A new generation FFDM/tomosynthesis fusion system with selenium detector. *Proc. of SPIE* 2010; 7622: 76220B1–76220B11
- 17 Ren B, Ruth C, Stein J et al. Design and performance analysis of the prototype full field breast tomosynthesis system with selenium based flat panel detector. *Proc. of SPIE* 2005; 5745: 550–561
- 18 Marshall NW, Bosmans H. Measurement of system sharpness for two digital breast tomosynthesis systems. *Phys Med. Biol* 2012; 57: 7629–7650
- 19 European Commission. European protocol for the quality control of the physical and technical aspects of mammography screening. In: European guidelines for quality assurance in breast cancer screening and diagnosis Fourth edn EUREF Luxembourg: European Commission; 2006
- 20 Samei E, Michael J, Flynn MJ et al. A method for measuring the presampled MTF of digital radiographic systems using an edge test device. *Med. Phys* 1998; 25: 102–113
- 21 Marshall NW, Monnin P, Bosmans H et al. Image quality assessment in digital mammography: part I. Technical characterization of the systems. *Phys Med. Biol* 2011; 56: 4201–4220
- 22 Marshall NW. Early experience in the use of quantitative image quality measurements for the quality assurance of full field digital mammography x-ray systems. *Phys Med. Biol* 2007; 52: 5545–5568
- 23 Marshall NW. Detective quantum efficiency measured as a function of energy for two full-field digital mammography systems. *Phys Med. Biol* 2009; 54: 2845–2861
- 24 NHSBSP (National Health Service Breast Screening Programme). Calculation of quantitative image quality parameters NHSBSP Equipment Report 0902. Sheffield: NHSBSP Publications; 2009
- 25 Neitzel U, Günther-Kohfahl S, Borasi G et al. Determination of the detective quantum efficiency of a digital x-ray detector: Comparison of three evaluations using a common image data set. *Med. Phys* 2004; 31: 2205–2211
- 26 Ayala R, García-Mollá R, Linares R. MIQuaELa, Image Quality Evaluation Laboratory (version 1.0). Madrid, Spain: HGUGM; 2009
- 27 Ayala R, Linares R, García-Mollá R. MIQuaELa, Software for DQE measuring in digital Radiography/Mammography. *IFMBE Proceedings* 2009; 25: 825–828
- 28 Yaffe MJ. Detectors for digital mammography. Bick U, Diekmann F (Eds.) *Digital Mammography 2010: 220*
- 29 Smith SW. *The Scientist and Engineer's Guide to Digital Signal Processing*. California, USA: California Technical Publishing; 2003: 89–91
- 30 Choi JG, Park HS, Kim YS et al. Characterization of prototype full-field breast tomosynthesis by using a CMOS array coupled with a columnar CsI(Tl) scintillator. *Journal of Korean Physical Society* 2012; 60: 521–526
- 31 Choi JG, Kim YS, Park HS et al. Evaluation of the clinical performance by using the effective DQE for a prototype digital breast tomosynthesis system. *Journal of Korean Physical Society* 2012; 60: 869–874